Article

pubs.acs.org/Biomac

Formulation and Composition Effects in Phase Transitions of Emulsions Costabilized by Cellulose Nanofibrils and an Ionic Surfactant

Siqi Huan,[†] Shingo Yokota,[‡] Long Bai,[†] Mariko Ago,[†] Maryam Borghei,[†] Tetsuo Kondo,[‡] and Orlando J. Rojas*[,†,§]

[†]Department of Bioproducts and Biosystems, School of Chemical Engineering, and [§]Department of Applied Physics, School of Science, Aalto University, P.O. Box 16300, FIN-00076 Aalto, Espoo, Finland

[‡]Graduate School of Bioresource and Bioenvironmental Sciences, Kyushu University, 6-10-1, Hakozaki, Higashi-ku, Fukuoka 812-8581, Japan

Supporting Information

ABSTRACT: Cellulose nanofibrils (CNF) offer great prospects as a natural stabilizer of colloidal dispersions and complex fluids for application in food, pharma, and cosmetics. In this study, an ionic surfactant (sodium dodecyl sulfate, SDS) was used as emulsifier of oil-in-water and water-in-oil emulsions that were further costabilized by addition of CNF. The adsorption properties of SDS in both, CNF dispersions and emulsions, as well as the influence of composition (CNF and SDS concentration) and formulation (ionic strength, oil, and CNF types) on the phase behavior were elucidated and described in the framework of Windsor systems. At low salinity, the phase transition of emulsions containing CNF and SDS at low concentrations was controlled by molecular transfer in the oil-in-water system. Irregular droplets and "bi-continuous" morphologies were observed at medium and high salinity for systems containing high CNF and SDS concentrations. Water-in-oil emulsions were only possible at high salinity and SDS concentrations in the presence of small amounts of CNF. The results revealed some subtle differences in CNF interfacial activity, depending on the method used for their isolation via fiber deconstruction, either from microfluidization or aqueous counter collision. Overall, we propose that the control of emulsion morphology and stability by addition of CNF opens the possibility of developing environmentally friendly complex systems that display high stability and respond to ionic strength following the expectations of classical emulsion systems.

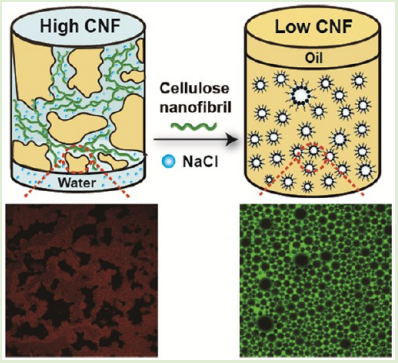

INTRODUCTION

Emulsification is a powerful technique for dispersing immiscible fluids within a continuous liquid phase.[1] Thermodynamically, emulsions are nonequilibrium systems in which macroscopic phase separation will eventually occur toward a lower free energy state; thus, they are complex metastable systems in kinetic equilibrium.[2] Emulsifiers are added in order to achieve emulsion stability and play important roles in emulsion formulation: they reduce the interfacial tension and protect the droplets from aggregation by generating steric or electrostatic repulsion.[3] A large number of natural and synthetic emulsifiers have been used.[4,5] Inorganic (silica, clay, and calcium carbonate),[6] and biobased (protein, starch, and cellulose) particles,[7,8] ranging in sizes from the nanometer to the micrometer scale, have been reported as efficient interfacial stabilizers, resulting in Pickering emulsions. Since the demands for developing sustainable materials are increasing, naturally derived particles are considered among the most promising candidates in particle-stabilized emulsions.[9] Lignin particles,[10−14] chitin nanocrystals,[15] chitosan,[16] and starch nanocrystals[17] and, especially, cellulose nanocrystals (CNC)[18−24] have been used for emulsion stabilization. Some few reports exist on the stabilizing ability of cellulose nanofibrils (CNF),[25−27] whose behavior at interfaces as well as interactions with surfactants have been reviewed recently and the reader is referred to the body of work cited therein.[28,29]

CNF extracted from abundant natural plant sources consist of long, flexible and entangled fibrils that readily gel in water and exhibit a reinforcing or strengthening effect in polymer composites.[30,31] The interfacial activity of CNF at oil/water interfaces enables its function as emulsion stabilizer but the degree at which stable emulsions are obtained depends on the oil type and other composition and formulation variables. For this reason, in some cases, CNF combination with a surfactant can lead to very highly stable oil-in-water (O/W) emulsions.[27] It is generally accepted that the presence of network-like aggregates comprising cellulose fibrils at the oil−water interface is a contributing factor preventing droplet coalescence.[32,33] Steric repulsion between droplets is expected in systems emulsified by nonionic surfactants and a small repulsion

Received: October 8, 2017
Revised: November 11, 2017
Published: November 13, 2017

DOI: 10.1021/acs.biomac.7b01452
Biomacromolecules 2017, 18, 4393−4404

between CNF and the surface of the droplets may produce stabilization effects.[27] Furthermore, the rheological behavior of mixtures containing diluted CNF dispersions and different nonionic surfactants points to the important role of related interactions.[34] In contrast, emulsions produced by ionic surfactants are stabilized by strong electrostatic repulsion between the droplets, which may be significantly affected by the addition of CNF, depending on the balance of electrostatic charges.[29]

In this study, an ionic surfactant (sodium dodecyl sulfate, SDS) was used in combination with two types of CNFs to stabilize emulsions and the phase inversion behavior of related systems was considered, which is most relevant in the preparation and application of emulsified products.[35] This included a study of the transitional phase inversion, which was initiated by changing the strength of interactions between the surfactant and the fluid phases. In this context, it is known that the interactions with nonionic surfactants are affected by temperature,[36] while those for ionic surfactants depend mainly on the ionic strength.[37,38] For example, at low salinity, the curvature of oil-water interface is concave toward the oil is favored (leading to O/W emulsions). However, the interaction between water and the hydrophilic or charged group in an ionic surfactant becomes unfavorable with the increased concentration of electrolyte in the aqueous phase. Therefore, a concave interface toward water is expected at high salinity (favoring W/O emulsions). Interfaces displaying low curvature are expected at intermediate salinity.[39] Emulsions at which this curvature inversion occurs are called bicontinuous emulsions, whereby oil and water can simultaneously be the continuous phase.[40]

Oil-continuous and bicontinuous emulsions are uncommon in systems containing unmodified, hydrophilic CNF, which normally forms water-continuous emulsions. In fact, the phase transition behavior of CNF-stabilized emulsions has not been investigated in detail. Therefore, this study addresses the effect of salinity on the phase transition behavior of CNF-containing emulsions. To our knowledge, this is a first attempt to uncover the effect of electrolyte in the phase behavior of surfactant−oil−water (SOW) systems and the ensuing response to electrolyte in CNF-stabilized emulsions. Remarkably, by changing the salinity, O/W, W/O, and bicontinuous-like emulsion systems were achieved depending on the emulsion stabilizer composition (CNF and SDS). As a demonstration, SDS was used in the presence or absence of CNF in emulsions that were prepared by simple mechanical blending of the fluid phases (oil and water). Our conclusions are expected to open new opportunities for the design and utilization of natural particles in the formulation of emulsion systems that undergo phase transitions, depending on the ionic strength and the nanofibril loading in the aqueous phase.

EXPERIMENTAL SECTION

Materials. Microcrystalline cellulose powder (MCC) was obtained from Funacel II, Funakoshi, Co., Ltd., Tokyo, Japan. Toluene, sodium dodecyl sulfate (SDS), sodium chloride (NaCl), pentanol, Nile red, and Calcofluor white were purchased from Sigma-Aldrich (Helsinki, Finland). Milli-Q water was purified with a Millipore Synergy UV unit (Milli-Q) and used throughout the experiments.

Preparation of CNF and ACC−CNF. Bleached sulphite fibers suspended in water (1.5% solids content) were used to produce CNF. The fibers were first processed under high shear in a Masuko Supermasscollider grinder after three passes, and then they were further fluidized by using a microfluidizer (M110P, Microfluidics Corp., Newton, MA) equipped with 200 and 100 μm chambers under 2000 psi for 12 passes. The morphology of the resultant CNF was characterized by atomic force microscopy (Figure S1a).

For comparison, a CNF type that is expected to be less hydrophilic, produced by the Aqueous Counter Collision method, termed herein as ACC−CNF,[41] was also utilized to study the emulsion phase transition behavior at various salinities. The process for preparation of ACC−CNF followed protocols reported previously.[42,43] Briefly, MCC was prerinsed in deionized water and acetone, following by stirring in deionized water for at least 30 min at room temperature before using vacuum filtration to remove water. After repetition for three times, the dispersion/filtration procedure was carried out using acetone (twice). The MCC was dried under vacuum condition at room temperature for at least 12 h. An aqueous counter collision (ACC) system (CNNT Co. Ltd., South Korea) was used to treat 1.0% (w/w) prerinsed MCC at an ejecting pressure of 200 MPa. This process was repeated for 60 cycles and then centrifuged (370 g, 10 min, 25 °C) to remove the residues with sizes in the microscale. The morphology of the prepared ACC−CNF is shown in Figure S1b. For simplicity, in the discussion we generally use the abbreviation "CNF" to refer to both types of nanocelluloses but indicate the specific case of ACC−CNF when applicable.

Emulsion Preparation. In the emulsions, toluene was used as the oil phase that was mixed with aqueous SDS solutions in the presence or absence of dispersed CNF. The oil-to-water ratio (WOR by volume) was 50:50. The stock suspension of CNF was first diluted to given concentration by addition of Milli-Q water. The component weight % used in this study is based on the mass of the aqueous phase. Briefly, the given amount of SDS was first added into the CNF aqueous suspension followed by water bath sonication for 5 min (Ultrasonic nominal output of 40W, DT 52/H, Sonorex Digitec, Bandelin, Berlin, Germany). To obtain the respective emulsion, the CNF/SDS mixture was blended with toluene by gentle hand-shaking, before using a high-speed mixer operated at 9000 rpm for 5 min (digital UltraTurrax, IKA, Germany). After preparation, emulsion samples were stored and equilibrated at ambient temperature for 24 h, before characterization.

Two composition variables were investigated in the CNF-stabilized emulsions: (a) SDS concentration (from 0.01 to 1.2 wt %) at fixed CNF content (0.1 wt %), and (b) CNF concentration (from 0 to 0.5 wt %) at fixed SDS concentration (0.3 wt %). Changes in ionic strength were applied as a formulation variable: the salt (NaCl) concentration was varied between 0 and 8.8 NaCl wt % at the given SDS (0.3 or 1.2 wt %) and CNF (0.1 or 0.5 wt %) concentrations. One mL of pentanol was added in the salinity scans that were carried out at 1.2 wt % SDS concentration. The alcohol reduced the rigidity of the interface and prevented the formation of liquid crystal phases.

Characterizations. Surface tension isotherms of SDS in both, CNF dispersions and emulsions, were obtained with a KSV Sigma 70 tensiometer (KSV Instruments Ltd. Finland). A glass cup that contained the given volume of CNF dispersion or emulsions was contacted with a Du Noüy ring positioned at air−liquid interface. The corresponding force to maintain the ring in place was monitored by a computer-controlled system and the corresponding surface tension was calculated. The electrical conductivity of the emulsion samples was measured with a conductivity meter (CG852, Schott, Germany).

The morphology of the cellulose nanofibers was assessed by using an atomic force microscope (AFM, Dimension Icon, Bruker, Billerica, MA, United States). Images were obtained under tapping mode at a scan rate of 0.999 Hz. Scanning was applied over large (25 μm × 25 μm) and small (3 μm × 3 or 5 μm × 5 μm) areas.

Confocal laser scanning microscopy (CLSM) images of the emulsions were acquired using a Leica DMRXE confocal microscope (Leica, Germany) equipped with a 20× objective. A drop of the emulsion sample was placed on a glass slide and then a cover slide was quickly placed on top of the sample. Double-side adhesives were placed between glass slides and used as a spacer, preventing compression of the cover slide on the sample. The oil phase was stained with Nile red (492/520 nm) before observation. A Leica DM4500 polarized optical microscope (POM) with 10× and 20×

DOI: 10.1021/acs.biomac.7b01452
Biomacromolecules 2017, 18, 4393−4404

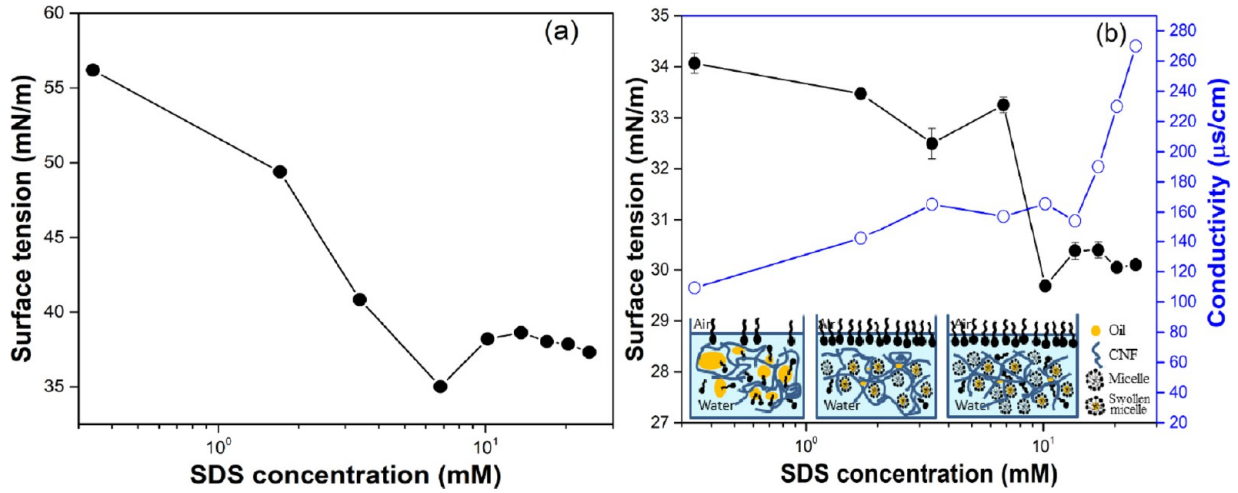

Figure 1. (a) Surface tension isotherm of SDS solutions at different concentrations in the presence of CNF (0.1 wt %). Note: the critical micelle concentration (CMC) of pure SDS in water is 8.1−8.2 mM. (b) Surface tension and conductivity of toluene-in-water emulsions produced with SDS in the presence of CNF (0.1 wt %). The inset shows a schematic illustration of SDS association with CNF and free micelles in the emulsions containing CNF.

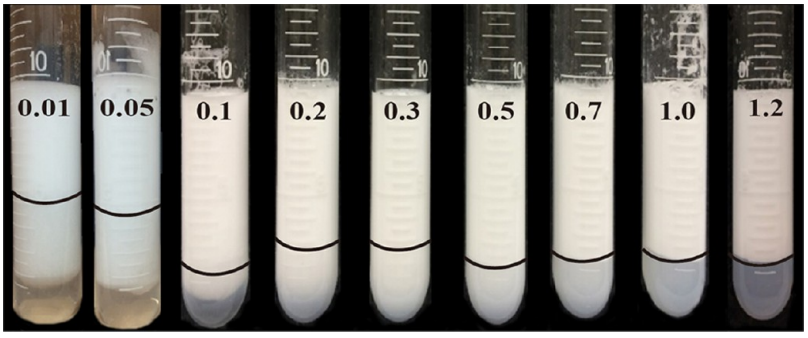

Figure 2. Visual appearance of surfactant−oil−water (SOW) systems (WOR = 1) prepared with SDS in the presence of CNF. The concentration (wt %) of SDS is indicated while that for CNF was kept constant at 0.1 wt %. The systems included an aqueous (bottom) as well as an opaque (middle) and upper emulsion phases. A black line in each tube was drawn for guidance to indicate the phase boundary between the emulsion (upper) phase and the excess, aqueous phase located underneath. Images of systems in the absence of SDS are included in the Figure S2.

objectives (Leica, Germany) was used to identify CNF in the emulsions. The observation mode in POM was changed from polarized to fluorescence by applying a blue illuminant. CNF was stained by Calcofluor white (365/435 nm) before imaging.

The mean droplet size of emulsions was determined by surface-weighted mean diameter (Sauter mean diameter, $d_{32} = \Sigma n_i d_i^3 / n_i d_i^2$) via Hydro 2000MU Mastersizer (Malvern, U.K.). Before size measurement, the emulsion sample was diluted with water in order to avoid multiple scattering. The refractive indices (RI) of the oil and aqueous phases used in the calculations were assumed to be 1.497 and 1.330, respectively.

The stability of the emulsions was characterized by the centrifugation method: the given sample was centrifuged at 3000 rpm for 5 min and the relative stability was calculated as the % volume that phase-separated.

RESULTS AND DISCUSSION

Surface Tension of CNF/SDS Aqueous Systems and Emulsions. The interfacial behavior of CNF/SDS systems was studied by tensiometry of the aqueous systems as well as the CNF-stabilized emulsions. Figure 1a includes the surface tension isotherm for SDS solutions in the presence of CNF (0.1% concentration). As expected, the surface tension was reduced with increasing SDS concentration and the critical aggregation concentration (CAC) was reached at 6.8 mM SDS in the system (equivalent to 0.2 wt % SDS in the aqueous phase). This value is slightly lower than the critical micelle concentration (CMC) of pure SDS in water (8.1−8.2 mM = 0.24 wt %).[44,45] Thus, it was apparent that the presence of CNF triggered surfactant association in the aqueous phase at SDS concentrations below its CMC. This may be the result of the interactions between the partially hydrophobic character of the cellulose fibrils and the alkane chain of SDS, leading to an increased local concentration of SDS molecules.[34,46] In contrast to the aqueous system, the CAC value of SDS in CNF-stabilized emulsions was higher, 10 mM (0.29 wt % SDS concentration), but showing lower surface tension at similar SDS concentrations. Upon addition of toluene and emulsion formation, the SDS molecules adsorbed at the water−toluene interface. The toluene droplets exhibited a large interfacial area, thereby a large number of SDS molecules were used for stabilization of the oil droplets, reducing the surface excess at the air−liquid interface. Moreover, the hydrophobic group of SDS is expected to have a strong affinity with toluene and less SDS molecules were available to interact with CNF, resulting in more nonassociated, free surfactant molecules. Alternatively, CNF may weaken hydrogen bonding in water molecules by establishing new intermolecular interactions with the hydroxyl group of CNF, which can decrease the surface tension at the

DOI: 10.1021/acs.biomac.7b01452
Biomacromolecules 2017, 18, 4393−4404

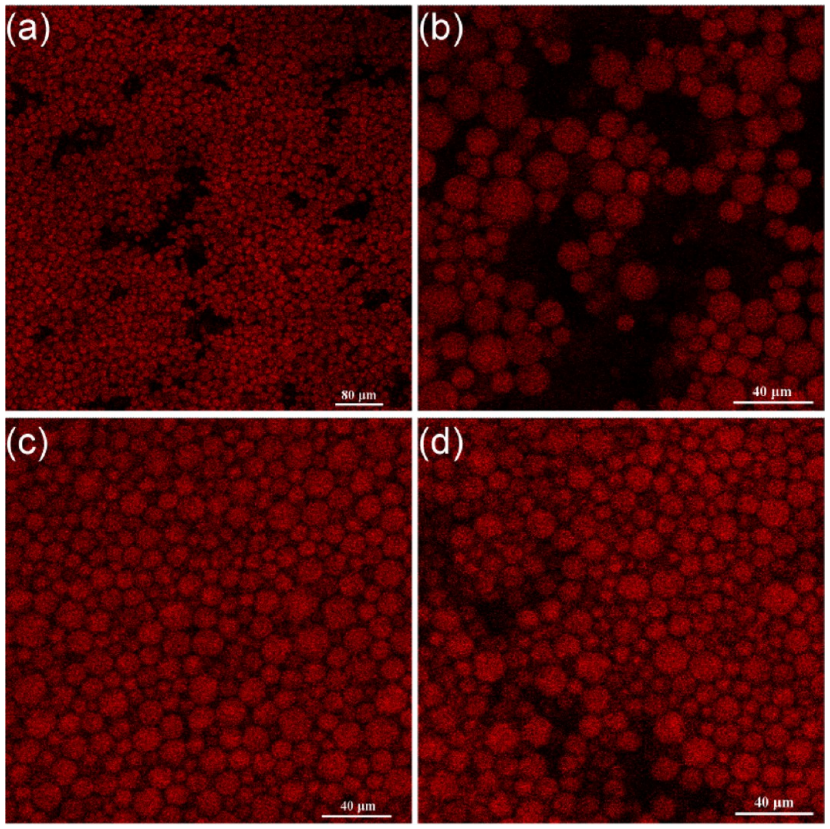

Figure 3. CLSM micrographs of emulsions produced with different SDS concentrations in the presence of CNF. The system with 0.1 wt % SDS is shown (a) at low and (b) high magnification. Included are also the emulsions prepared with (c) 0.3 wt % and (d) 0.7 wt % SDS. The CNF concentration was kept constant at 0.1 wt %. The oil phase was stained with Nile red. The prepared emulsions were stored at ambient conditions for 24 h before imaging. The scale bar in the images correspond to 80 μm in (a) and 40 μm for the rest of the images (b)−(d).

water−air interface. Accordingly, a schematic illustration of micelle formation of SDS in CNF-stabilized emulsions is proposed in Figure 1b. It is reasonable to propose that the increased CAC in CNF-stabilized emulsions and lower surface tension compared with pure SDS system is affected by the reduced interfacial tension at water−toluene interface and by the disruption of the interaction between CNF and SDS molecules. Interestingly, conductivity measurements in the same systems showed a plateau below the CAC, which is possibly caused by insufficient surface coverage of toluene droplets, or by the influence of the surface charge of CNF. Finally, we note that except for small changes in the association concentration, similar behaviors were observed for ACC−CNF.

Effect of SDS Ionic Surfactant. The concentration of SDS plays a key role in emulsification ability and the ensuing morphology of the emulsion. CNF-stabilized emulsions prepared at different SDS concentrations were investigated at constant CNF loading (0.1 wt %; Figure 2). After emulsification and equilibration for 24 h, all emulsions were observed to be stable (no coalescence was apparent) and demonstrated the stabilization ability of CNF. However, in the absence of SDS, phase separation happened shortly after preparation of the CNF-containing emulsions, even at CNF concentrations as high as 0.5 wt % (Figure S2). This was also observed in the case of emulsions prepared with CNC.[47,48] The effect of SDS concentration on the emulsion phase behavior is shown in Figure 2: three phases separated when the concentration of SDS was below the CMC or CAC (0.01 to 0.2 wt %). The phases consisted of an excess aqueous phase (bottom) as well as an opaque (middle) and upper emulsion phases. By gradually increasing the SDS concentration, the volume of the aqueous phase was reduced and turned more turbid. At higher SDS concentrations (>0.3 wt %), two separated phases were observed (the aqueous phase in the bottom and the upper, emulsion phase). Interestingly, the volume of the aqueous phase remained nearly constant and became more translucent with further increase in the SDS concentration, indicating that high SDS concentrations were effective in stabilizing the emulsions.

Figure 3 includes the CLSM micrographs of emulsions stabilized in the presence of CNF at different SDS concentrations (below, at and above the CAC). Uniform, spherical droplets are observed, with diameters in the micron size range, typical of stable emulsions with a large volume of the organic (oil) phase. From Figure 3a,b, it can be inferred that the presence of CNF favored the stabilization of the oil droplets and prevented flocculation and coalescence. One possible reason for this observation is that, despite the fact that charges of the same sign exist for both CNF and SDS, the CNF formed network-like structures in the aqueous phase, increasing the viscosity, thereby increasing the toluene−water interface stability, even at low SDS concentration.[25] Furthermore, at an increased SDS concentration, from 0.3 to 0.7 wt %, the droplet size remained quite similar than that observed at lower concentrations (Figure 3c,d). Confirmation can be found in Table S1 of the Supporting Information, which indicate droplet sizes between 11 and 13 μm. The oil droplet size observed in this work was smaller compared to that measured by Gestranius

DOI: 10.1021/acs.biomac.7b01452
Biomacromolecules 2017, 18, 4393−4404

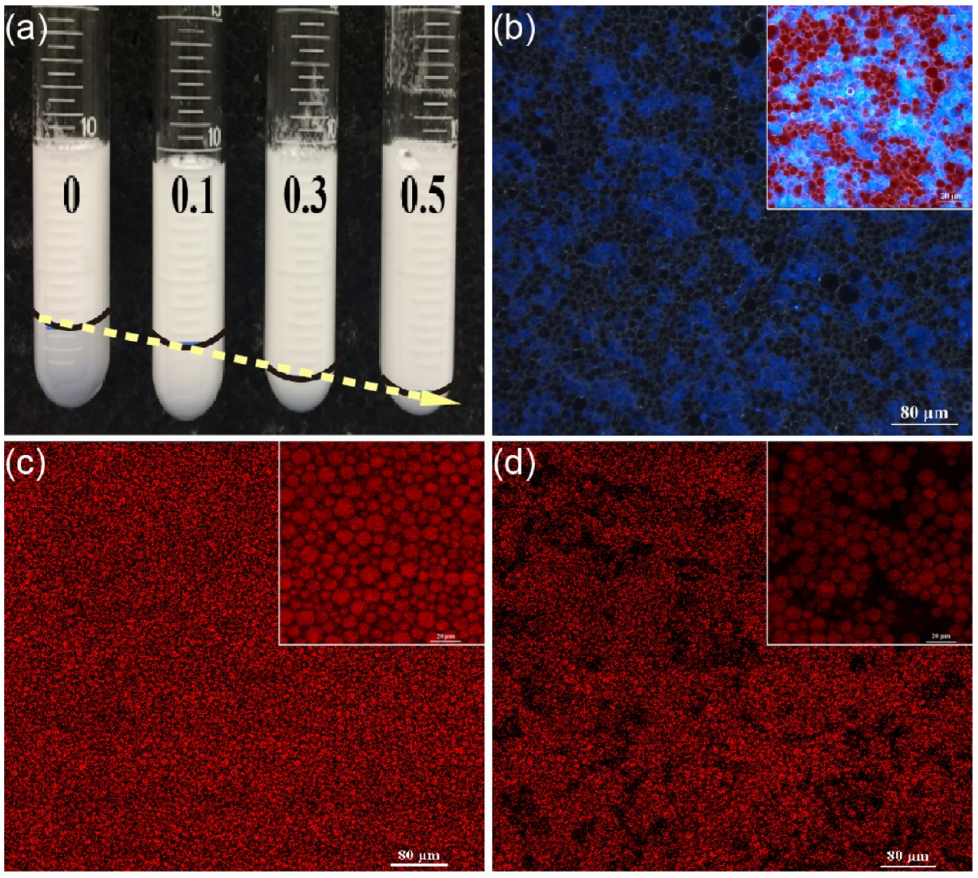

Figure 4. (a) Photos of test tubes containing oil-in-water emulsions (WOR = 1) at different CNF concentrations in the aqueous phase (wt % as indicated), and after 24 h equilibration. The concentration of SDS was kept constant at 0.3 wt %. The black line drawn on each tube indicates the interfacial boundary between the phases. (b) Polarized optical microscope image of CNF-loaded emulsions (0.3 wt %), indicating the location of CNF in the emulsion. CNF was identified with Calcofluor white. CLSM micrographs of emulsions also included in (c) in the absence and (d) in the presence of 0.5 wt % CNF. The scale bar in (b)−(d) is 80 μm. The inset images in (b), (c), and (d) are micrographs taken with larger magnification, 20 μm scale bar. The oil phase was stained with Nile red. The prepared emulsions were stored at ambient conditions for 24 h before imaging.

et al., ∼20 μm, for surfactant-free dodecane-in-water emulsions stabilized by CNF at >1 wt % concentration.[49] Note, however, that in this work the volume of oil phase was 20 wt % and the emulsions creamed easily, with a high density of droplet clusters. Taken together, it can be concluded that emulsions prepared with SDS, in the presence of CNF, can be obtained efficiently by simply blending the oil and aqueous phases, resulting in stable and uniform small droplets.

For further investigating the stability of the emulsions, samples prepared with 0.1, 0.3, 0.5, and 0.7 wt % SDS were centrifuged at 3000 rpm for 5 min. The emulsion volume fraction that separated after centrifugation was determined and reported in Table S1. Such fractions corresponded to 9.4, 37.5, 43.8, and 44.1% at SDS concentrations of 0.1, 0.3, 0.5, and 0.7 wt %, respectively. The results highlight the role of SDS concentration on the stability of the emulsions.

Emulsion Stabilization with CNF. We turn our attention to the influence of CNF on emulsions prepared with SDS at 0.3 wt %. This SDS concentration was chosen according to the previous results indicating that CAC of SDS was ∼0.3 wt %, at which a minimum amount of free surfactant exists in solution. The phase behavior studies also indicated that no major differences existed in the emulsions prepared at SDS concentrations > CAC. Figure 4a includes images of O/W emulsions formulated with different CNF loadings (0, 0.1, 0.3, and 0.5%). In the absence of CNF, there was a larger excess of the bottom, aqueous phase while the addition of CNF clearly reduced the volume that phase-separated, i.e., increased the volume of the emulsified fraction. Hydration effects and CNF in emulsion samples may be reasons for these observations, namely, water molecules adsorbed onto the surface of CNF, forming a network via hydrogen bonding interactions, which increased the viscosity and stabilized the oil droplets in the continuous, aqueous phase. In order to better identify the role and location of CNF in the emulsions, the cellulose nanofibrils were stained with Calcofluor white and observed under a polarized microscope. As presented in Figure 4b, the fibrils were located in the aqueous phase, around the oil droplets. This points to the stabilizing mechanism of CNF, which might be the result of the synergistic effect of the long flexible chains, the negative surface charge and the formation of a fibril network. Figure 4c,d compares the oil droplet morphology in the absence and presence of CNF (0.5 wt %). Uniform oil droplet sizes were observed for both conditions, while the clustering of the oil droplets was somewhat different (compare oil droplets in Figure 4c,d). However, this can be an artifact from sample preparation or from the free volume that was reduced in the presence of CNF. In sum, with increased CNF concentration, toluene was emulsified more effectively and less (excess) water phase separated.

The droplet diameters of CNF-loaded emulsions are presented in Table S2. Comparatively larger oil droplet sizes

DOI: 10.1021/acs.biomac.7b01452
Biomacromolecules 2017, 18, 4393−4404

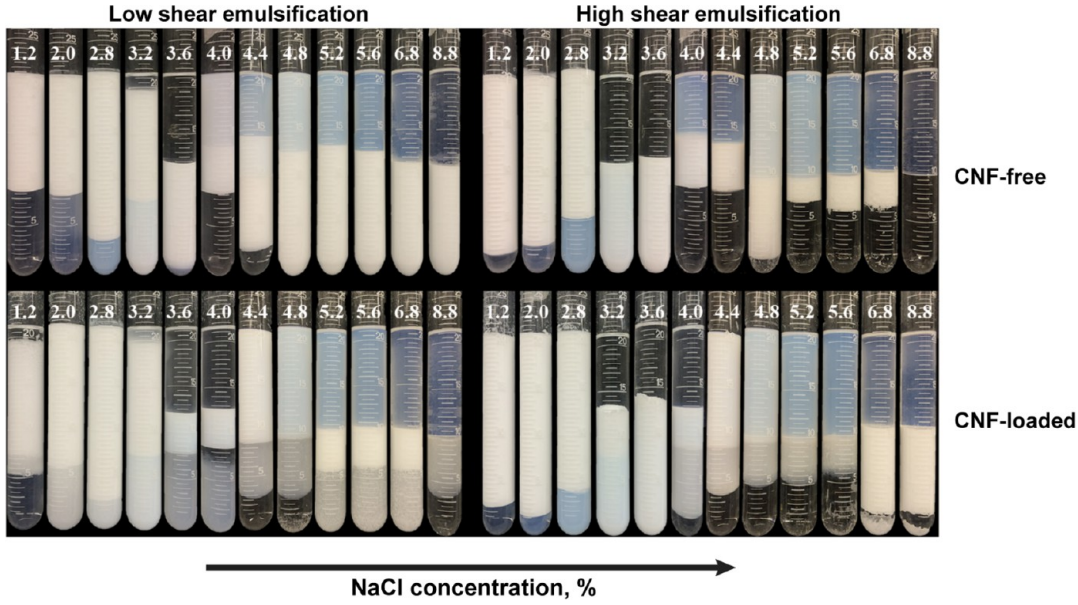

Figure 5. Salinity scans for SOW systems with SDS and toluene (WOR = 1). Photographs were taken after low shear (gentle) mixing by manually turning the test tubes around few times (labeled as "Low Shear Emulsification") and after emulsification by mechanical stirring (labeled as "High Shear Emulsification") in the absence (top row) and presence (bottom row) of CNF. The concentration of SDS and CNF were 1.2 and 0.1 wt %, respectively. Pentanol was added to prevent the formation of liquid crystal phases. The prepared emulsions were stored at ambient conditions for 24 h before observation.

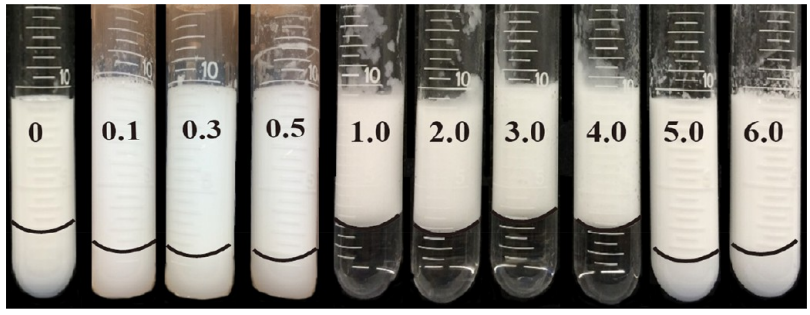

Figure 6. Visual appearance of emulsions (WOR = 1) prepared with given NaCl concentrations (wt %, as indicated). The concentration of SDS and CNF were 0.3 and 0.1 wt %, respectively. The black line drawn on each tube indicates the interfacial boundary between two adjacent phases (more difficult to appreciate in the photo than by direct visual observation). The prepared emulsion samples were stored at ambient for 24 h before characterization.

were measured in the absence of CNF, d_{32} of about ~14 μm. The d_{32} became smaller and the distribution of oil droplet size narrower with increasing CNF concentration (~6 μm at 0.5 wt % CNF). This result can be ascribed to the negative charges in CNF, which leads to strong electrostatic repulsion between oil droplets (CNF is distributed in the aqueous phase surrounding the oil droplets). It is possible that CNF formed an interfacial layer around the oil droplets. At an increased CNF concentration, a higher interfacial coverage around the oil droplets occurred, effectively, reducing the droplet size.[50] Overall, the addition of CNF both decreased the size and led to more uniform and stable oil droplets, clearly indicating better emulsification and interfacial stabilization.

Salinity and Phase Behavior of CNF-Stabilized Emulsions. Salinity scans of SOW systems were carried out after being subjected to low shear (gentle) and high shear (strong) emulsification. We note that in these systems thermodynamic equilibrium is not achieved and conditions closer to equilibrium, most relevant to studies of phase behavior, would require very little fluid exchange while the surfactant diffuses to the phase where it attains minimum free energy. Additionally, the presence of CNF obscured the identification of the different phases, given the increased light scattering and turbidity it produced. Nevertheless, some general conclusions can be derived from these scans where the two levels of applied mixing can shed light about the phase behavior and, in addition, give good indication of the properties of the emulsions formed. Keeping these considerations in mind, we compared the salinity scans for CNF-free and CNF-loaded systems (Figure 5). For both systems, it can be observed that after low shear mixing, a phase transition started to occur at a salt concentration of 3.2%, where excess oil phase began to form (and three phases were observed). For emulsions produced at high shear, these observations also held, despite the fact that the three phases were still present at NaCl concentrations as high as 6.8% (CNF-free systems). Obviously, the fact that the systems were emulsified, as evidenced by the presence of the opaque, white phase, made the analysis somewhat difficult.

DOI: 10.1021/acs.biomac.7b01452
Biomacromolecules 2017, 18, 4393−4404

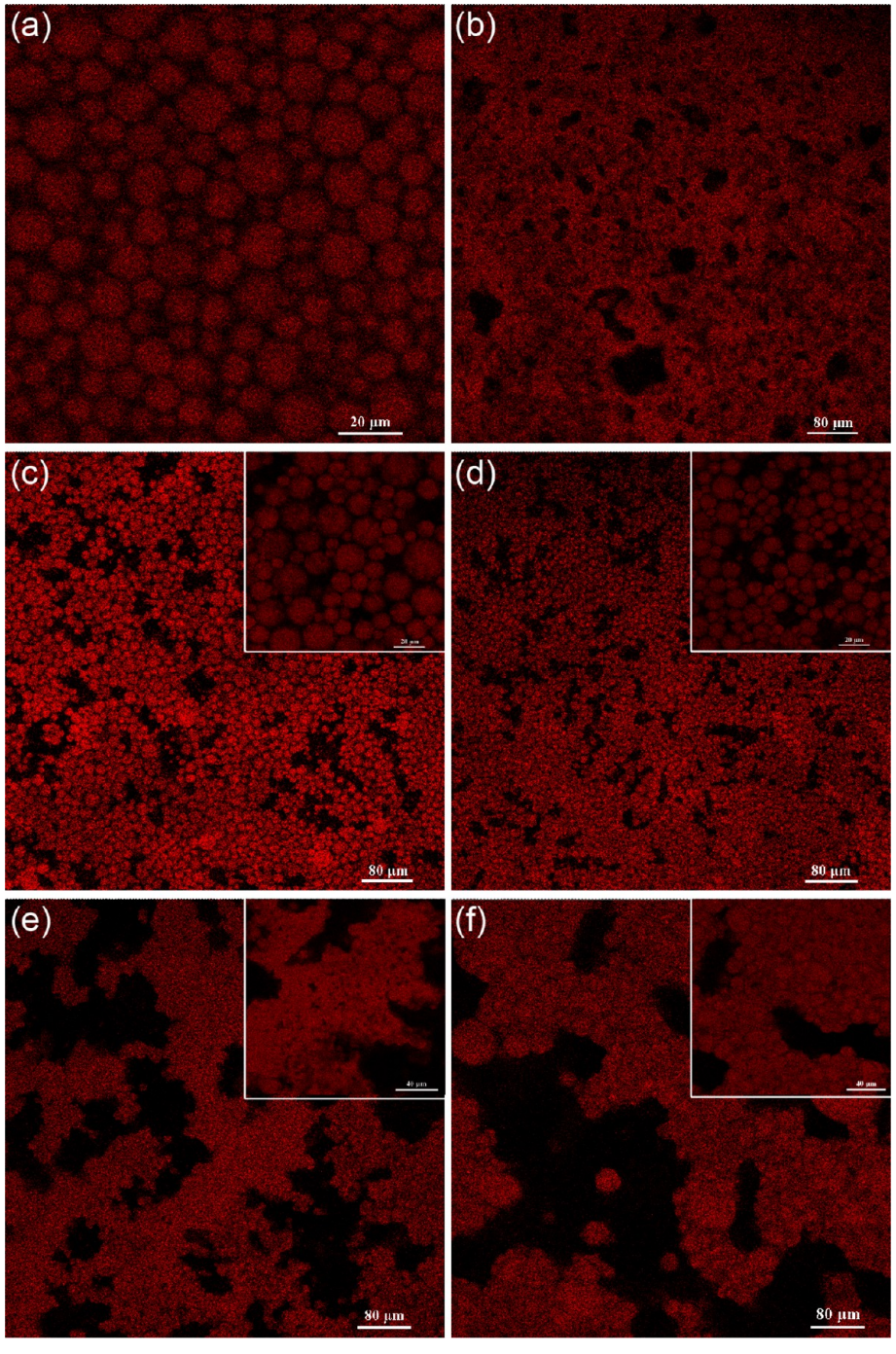

Figure 7. CLSM micrographs of CNF-free emulsions produced at a NaCl concentration of (a) 1 wt % and (b) 5 wt %. The concentration of SDS was 0.3 wt %. CLSM micrographs of CNF-loaded emulsions with different salt concentrations are also shown in (c) 0, (d) 1 wt %, (e) 3 wt %, and (f) 5 wt %. The concentration of SDS and CNF were 0.3 and 0.1 wt %, respectively. The scale bars correspond to 20 μm in (a) and 80 μm in (b)−(f). The insets in (c)−(f) correspond to larger magnification (scale bars of 20 or 40 μm, respectively). The oil phase was stained with Nile red. The prepared emulsion samples were stored at ambient conditions for 24 h before imaging.

At low salt concentration, the surfactant had a higher affinity with the water phase (Winsor I system) and produced O/W emulsions of a density lower than that of water. Thus, a cream layer atop the excess water was formed (see white phase in the test tubes). Above the transition concentration (or the so-called optimum salinity), the affinity of the surfactant with the oil was higher compared to that with water (Winsor II), and W/O emulsions were formed, with a density higher than that of the oil phase and thus, they settled in the bottom of the test tubes. These observations are evident for both salinity scans, after gentle and strong emulsification.

Similar observations as those presented so far apply for other oils (Figure S3). Unfortunately, for the CNF-free SOW scans, it was difficult to identify the formation of a three-phase system (Winsor III), which would include a bicontinuous middle phase at the optimum salinity. This is simply explained by the fact that emulsification occurred readily and evolution to fully phase-separated systems would take a long time. The system turned

DOI: 10.1021/acs.biomac.7b01452
Biomacromolecules 2017, 18, 4393−4404

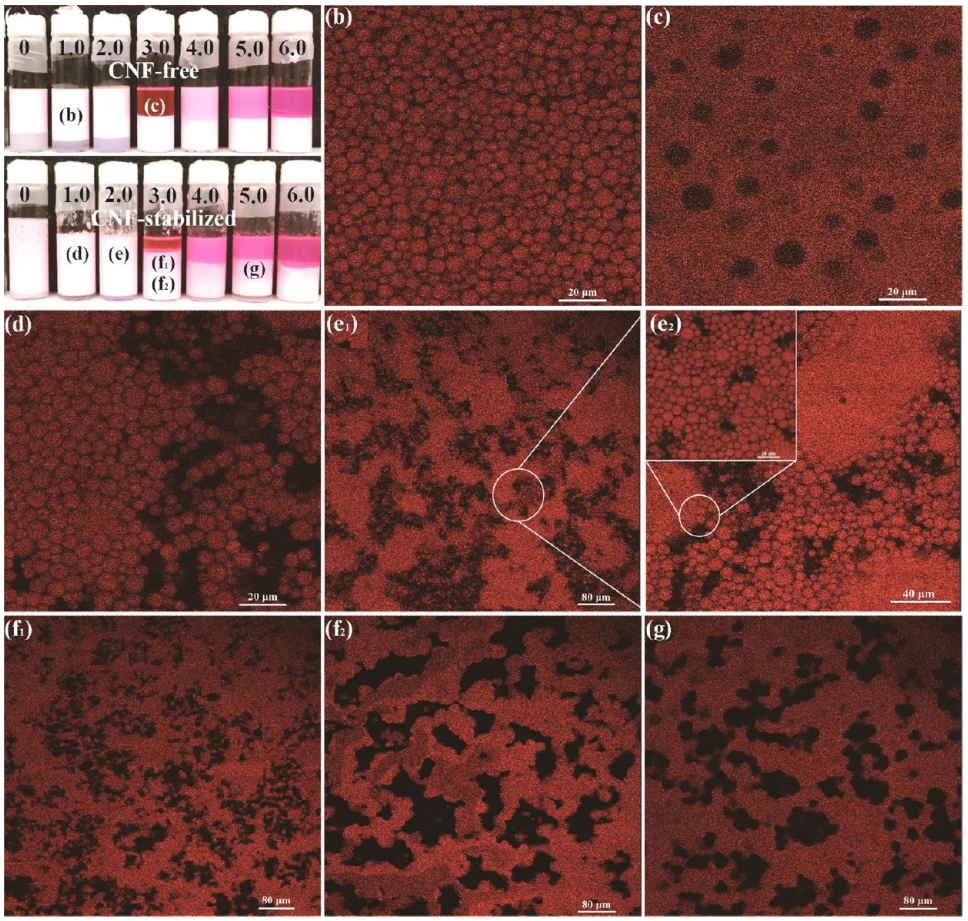

Figure 8. (a) Visual appearance of toluene-in-water emulsions (WOR = 1) with different salinities (wt %). The concentration of SDS and CNF were 1.2 and 0.5 wt %, respectively. Pentanol was added to prevent the formation of liquid crystal phases. CLSM micrographs of CNF-free emulsions with (b) 1 wt % NaCl (showing a O/W or normal emulsion) and (c) 3 wt % (showing W/O or inverted emulsions). CLSM micrographs of emulsions in the presence of CNF are also included for salt concentration of (d) 1 wt %, (e_1, e_2) 2 wt %, (f_1, f_2) 3 wt %, and (g) 5 wt %. (e_2) Enlarged areas from (e_1). The oil phase was stained with Nile red. The prepared emulsion samples were stored at ambient conditions for 24 h before imaging.

from Winsor I (<3.6 wt %) to Winsor II (>4 wt %) with the corresponding emulsions changing from O/W to W/O.

In order to investigate the phase behavior of SOW systems in the presence of CNF, and for various salinities, emulsions with extreme SDS and CNF concentrations were prepared, namely, a set with 0.3 wt % SDS and 0.1 wt % CNF concentration (Figures 6 and 7) were compared against another set produced with 1.2 wt % SDS and 0.5 wt % CNF (Figure 8). Figure 6 shows the emulsions prepared with the first set. Here, it is interesting to note that the phase at the bottom of the test tubes turned clear when the NaCl concentration reached 1 wt %. They then turned turbid again at higher salt concentrations (5 and 6 wt %). The reasons for these observations are not obvious, but they are likely related to the possible onset of phase inversion at high NaCl concentration, as will be discussed next.

CLSM micrographs shown in Figure 7 indicate details of the phase behavior, with and without CNF at various NaCl concentrations. In CNF-free systems, Winsor I systems, where the surfactant had a strong affinity to the aqueous phase, led to O/W emulsions. This also applied to systems in the presence of CNF (Figure 7a,c,d). Figure 7 clearly shows the occurrence of phase inversion (from water-continuous to oil-continuous systems) if CNF-free systems with 1 wt % (Figure 7a) and 5 wt % (Figure 7b) salt concentration are compared. In the latter case, corresponding to W/O emulsions, the water droplets were not distributed uniformly and were irregular in shape. This is likely because the concentration of SDS was too low and the possible effects of SDS aggregation at high salinity. The charged hydrophilic head of SDS molecules adsorbed at the interface to form O/W structures at low salt concentration. A change into the opposite morphologies occurred after the salinity reached the optimal value, thereby reversing the initially concave curvature of the oil−water interface, forming W/O emulsions. Figure 7c−f shows the changes of CNF-stabilized emulsions as a function of salinity, ranging from 0 to 5 wt %. Comparing Figure 7c (0% NaCl) and Figure 7d (1% NaCl), no obvious differences between the emulsions were apparent. Note, however, that the diameter of oil droplets decreased in the presence of salt (see Table S3). By further increasing the salinity to 3 wt % or to 5 wt %, the systems displayed more complex morphologies (Figure 7e,f). A clear phase inversion typical of W/O structures was not obvious since oil droplets still appeared to exist. It is expected that CNF prevented the phase transition process owing to its very hydrophilic nature, the network structure it forms and the increased viscosity of the aqueous phase, which favored water-continuous systems and a high water holding capacity, even in conditions where the transition process in CNF-free systems, with SDS molecules would have occurred already. As a result, instead of forming the

DOI: 10.1021/acs.biomac.7b01452
Biomacromolecules 2017, 18, 4393−4404

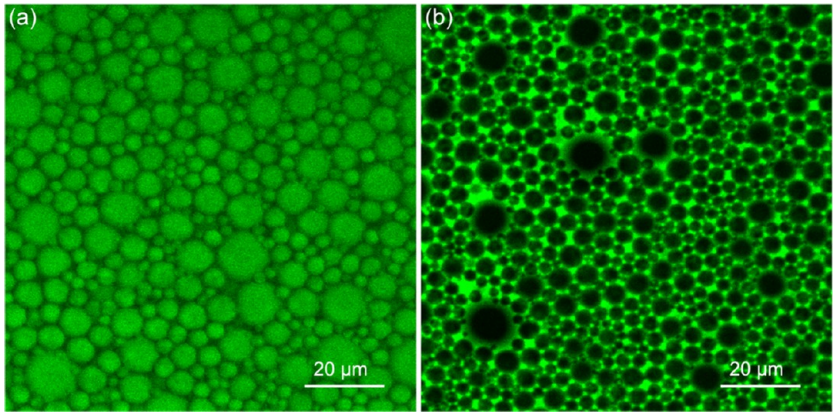

Figure 9. CLSM micrographs of toluene-in-water emulsion (WOR = 1) with (a) 2.8 wt % NaCl (O/W emulsion) and water-in-toluene emulsion with (b) 6.8 wt % NaCl (W/O emulsion). The concentration of SDS and CNF were 1.2 and 0.1 wt %, respectively. The oil phase was stained with Nile red and showed green. The prepared emulsion samples were stored at ambient conditions for 24 h before imaging.

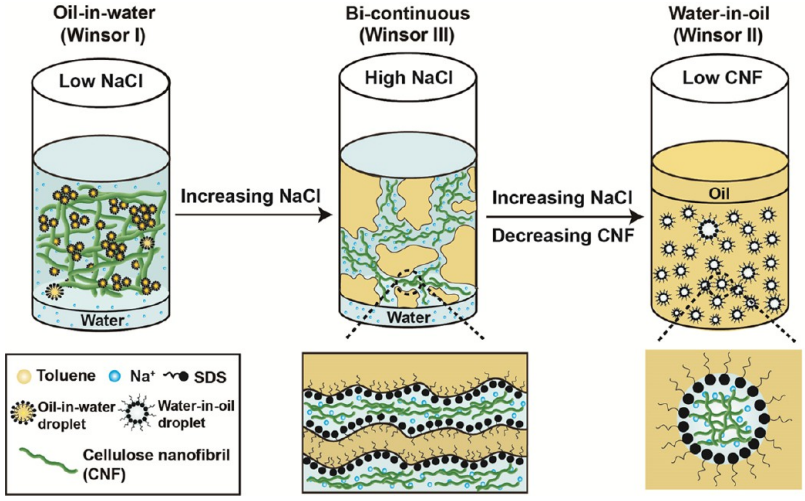

Figure 10. Schematic illustration explaining the observed phase transition behavior of emulsions prepared with SDS in the presence of CNF and at increased salinity. A possible morphology for intermediate NaCl concentrations is proposed. Note: the components are not drawn to scale, but shown with the given sizes for better clarity.

expected morphology (inverted or W/O emulsions), an irregular morphology with coexisting phases and large CNF/water phase domains (bicontinuous like) was formed (see Figures 7f and S4). The observations indicate the types of interactions and the fact that the amount of surfactant was not sufficient to stabilize effectively the interfaces under these conditions (see also Figure 1 and related discussion).

A set of emulsions prepared at high SDS and CNF concentrations are discussed next. The oil phase was prestained with Nile red in order to better characterize oil phase behavior. It can be clearly seen that for CNF-free emulsions, phase inversion occurred at a NaCl concentration of 2−3 wt % (Figure 8a). From confocal micrographs of these CNF-free emulsions (Figure 8b), O/W or normal emulsions with uniform oil droplets were obtained in the presence of 1 wt % salt. In contrast, inversion occurred (W/O emulsions were formed) at a higher salt concentration, 3 wt % (Figure 8c). Unlike the oil-continuous emulsion that displayed irregular aqueous morphologies at low SDS concentration (Figure 7b), the emulsions prepared at high SDS concentration showed regular water droplets, spherical in shape and uniform in size. For CNF-loaded emulsions, the phase transition occurred at a salinity of 2−3 wt %. Most interestingly, at higher salinities, three different phases were formed (excess oil in the upper layer, middle and bottom emulsion phases). These phases existed throughout the salinity scan. In confocal micrographs, uniform O/W droplets were observed at 1 wt % salinity (Figure 8d). However, in Figure 8e_1, corresponding to an O/W emulsion, the oil droplets were clustered together, forming aggregates (see also enlarged areas in Figure 8e_2). Figure 8f_1,f_2 correspond to the confocal micrographs of two different phases in the emulsion at the phase transition (optimum) salinity (3 wt %). It appears that a bicontinuous-tike system was formed. With further increasing salinity to 5 wt % (Figure 8g), such morphology was still present. However, from Figure 8f_1, f_2, and g, such structure at high SDS and CNF concentrations was finer compared to that observed at low concentrations (Figure 7f). On one hand, the higher CNF loading may have prevented phase transition. At high SDS and CNF concentrations, a much lower interfacial tension existed, leading to less coalescence of the water phase. Furthermore, high CNF concentrations may have also promoted a reduced interfacial tension at the water−oil interface by the effect of the interaction between CNF and water molecules via hydrogen bonding. Taken together, it can be concluded that addition of hydrophilic CNF produced emulsions with different phase morphologies while the phase

DOI: 10.1021/acs.biomac.7b01452
Biomacromolecules 2017, 18, 4393−4404

transition correlated with expectations of the effect of electrolyte as the formulation variable (salinity scans).

At high salinity, the emulsion systems with low or high concentrations of both CNF and SDS could not transition from O/W to W/O morphologies, which could be attributed to the stabilizing effect of unmodified, hydrophilic CNF. Following, emulsions were prepared with low CNF and high SDS concentrations to reveal the phase transition behavior as a function of the salinity.

A salinity scan with 0.1 wt % CNF and 1.2 wt % SDS was performed, as shown in Figure 5. From this scan, it is apparent that the phase behavior was very similar, below 2.8 wt % NaCl concentration. A variation took place over a salinity range around the optimal formulation, between 3.2 and 5.6 wt %, and it was similar after reaching 6.8 wt %. Accordingly, after high shear emulsification, phase transitions seemed to occur at NaCl concentrations of 2.8 and 6.8 wt %. Thus, emulsions at these salinities were investigated by CLSM, see Figure 9. O/W emulsions were formed at low salinity (Figure 9a), as discussed above; however, at an increased NaCl concentration, W/O emulsions with well-dispersed spherical droplets were obtained (Figure 9b). The diameter of water droplets was around 3−10 μm, indicating an efficient emulsification in CNF-loaded systems. The electrical conductivities of emulsions at 2.8 wt % NaCl and 6.8 wt % NaCl were 7 and 0.7 mS/cm, respectively, confirming the phase transition from O/W, at low salinity, to W/O at high salinity. These observations can be explained by the more limited stabilizing effect of CNF, which would otherwise favor water as the continuous phase. Thus, the role of SDS was dominant, leading to inverted, oil-continuous emulsions at high salinity. A schematic illustration summarizing the phase transition behavior of CNF-loaded emulsions is shown in Figure 10. The response to electrolyte addition in systems emulsified by ionic surfactant and costabilized by unmodified, hydrophilic CNF was realized while the amount of both surfactant and CNF determined the emulsion type.

So far we have revealed the transition process for oil-in-water to water-in-oil in compositions consisting of SDS and hydrophilic CNF. Here, the nature of the interactions between CNF and SDS, as induced by salt, plays a role in the phase behavior after emulsion preparation. Such detail effects remain for elucidation but are expected to involve electrostatic and hydrophobic effects. Finally, it is still interesting to understand the universality of related systems for a different type of CNF. As such, the salinity scan and CLSM images of emulsion phase transition (O/W to W/O) costabilized by a less hydrophilic CNF, namely, ACC−CNF, are shown in Supporting Information (Figures S5 and S6). The results indicate the applicability of the ACC−CNF in controlling the phase transition behavior since both oil-in-water and water-in-oil emulsions were produced. Interestingly, the water-in-oil droplet distribution for systems containing ACC−CNF was non-homogeneous at high salinity, indicating a limited capability in stabilizing the water droplets, which may be taken as a result of the ACC−CNF nanocelluloses employed, which is less hydrophilic than CNF. We note that competitive adsorption could have also affected the function of SDS molecules in stabilizing oil-continuous emulsions.

CONCLUSIONS

Emulsions of different morphologies were successfully obtained by simply blending oil and aqueous phases in the presence of a surfactant and a biobased costabilizer, CNF. SDS molecules showed different interfacial properties in CNF dispersions and CNF-stabilized emulsions. In emulsions, CNF was mainly present in the aqueous phase while SDS played a major role in oil droplet stabilization. The results demonstrated that despite the fact that SDS and CNF bare charges of similar sign, oil-in-water emulsions are easily obtained over a wide range of CNF and SDS concentrations. The main function of CNF in stabilizing oil droplets originated from the synergetic effect of long fibrous chains, negative surface charge and the network-like structure formed. The phase transition behavior was mainly controlled by salinity, transitioning from an oil-in-water to a water-in-oil system at increased salinity with irregular droplet morphologies at intermediate concentrations. At high salinity, a bicontinuous-like system was observed and water-in-oil emulsions were obtained at low CNF concentrations. The results are similar for other types of nanocelluloses, such as ACC−CNF, but reveal differences owing to the different hydrophilicity. This research opens a new avenue for the design and utilization of natural cellulose-derived materials to fabricating particle-stabilized emulsion systems that are responsive to changes in ionic strength.

ASSOCIATED CONTENT

Supporting Information

The Supporting Information is available free of charge on the ACS Publications website at DOI: 10.1021/acs.biomac.7b01452.

Additional materials are provided related to CNF morphology; the visual appearance of water/toluene systems in the absence of SDS; the salinity scan of water/octane in the absence and the presence of CNF; POM images of the bicontinuous-like emulsion; the salinity scan and CLSM images of ACC−CNF emulsion; and droplet sizes with different SDS, CNF concentrations, and salinities (PDF).

AUTHOR INFORMATION

Corresponding Author

*E-mail: orlando.rojas@aalto.fi. Tel.: +358-(0)50 512 4227.

ORCID

Mariko Ago: 0000-0001-5258-4624

Tetsuo Kondo: 0000-0003-4366-2955

Orlando J. Rojas: 0000-0003-4036-4020

Notes

The authors declare no competing financial interest.

ACKNOWLEDGMENTS

The Chinese Scholarship Council is acknowledged for support during the exchange of S.H. in Aalto University. We are grateful to the Academy of Finland for funding support through its Centres of Excellence Programme (2014-2019) and under Project 132723612 (HYBER).

REFERENCES

(1) McClements, D. J. *Food Emulsions: Principles, Practices, and Techniques*, 2nd ed.; CRC Press: Boca Raton, Florida, U.S.A., 2015; p 245.

(2) Chern, C. Emulsion polymerization mechanisms and kinetics. *Prog. Polym. Sci.* **2006**, *31*, 443−486.

(3) Bai, L.; Huan, S.; Gu, J.; McClements, D. J. Fabrication of oil-in-water nanoemulsions by dual-channel microfluidization using natural

DOI: 10.1021/acs.biomac.7b01452
Biomacromolecules 2017, 18, 4393−4404

emulsifiers: Saponins, phospholipids, proteins, and polysaccharides. *Food Hydrocolloids* **2016**, *61*, 703−711.
(4) McClements, D. J.; Bai, L.; Chung, C. Recent Advances in the Utilization of Natural Emulsifiers to Form and Stabilize Emulsions. *Annu. Rev. Food Sci. Technol.* **2017**, *8*, 205−236.
(5) Bai, L.; Huan, S.; Li, Z.; McClements, D. J. Comparison of emulsifying properties of food-grade polysaccharides in oil-in-water emulsions: Gum arabic, beet pectin, and corn fiber gum. *Food Hydrocolloids* **2017**, *66*, 144−153.
(6) Aveyard, R.; Binks, B. P.; Clint, J. H. Emulsions stabilised solely by colloidal particles. *Adv. Colloid Interface Sci.* **2003**, *100*, 503−546.
(7) Berton-Carabin, C. C.; Schroën, K. Pickering emulsions for food applications: background, trends, and challenges. *Annu. Rev. Food Sci. Technol.* **2015**, *6*, 263−297.
(8) Zoppe, J. O.; Osterberg, M.; Venditti, R. A.; Laine, J.; Rojas, O. J. Surface interaction forces of cellulose nanocrystals grafted with thermoresponsive polymer brushes. *Biomacromolecules* **2011**, *12*, 2788−2796.
(9) Pei, X.; Tan, Y.; Xu, K.; Liu, C.; Lu, C.; Wang, P. Pickering polymerization of styrene stabilized by starch-based nanospheres. *Polym. Chem.* **2016**, *7*, 3325−3333.
(10) Li, S.; Willoughby, J. A.; Rojas, O. J. Oil-in-Water Emulsions Stabilized by Carboxymethylated Lignins: Properties and Energy Prospects. *ChemSusChem* **2016**, *9*, 2460−2469.
(11) Ago, M.; Huan, S.; Borghei, M.; Raula, J.; Kauppinen, E. I.; Rojas, O. J. High-Throughput Synthesis of Lignin Particles (∼ 30 nm to ∼ 2 μm) via Aerosol Flow Reactor: Size Fractionation and Utilization in Pickering Emulsions. *ACS Appl. Mater. Interfaces* **2016**, *8*, 23302−23310.
(12) Li, S.; Ogunkoya, D.; Fang, T.; Willoughby, J.; Rojas, O. J. Carboxymethylated lignins with low surface tension toward low viscosity and highly stable emulsions of crude bitumen and refined oils. *J. Colloid Interface Sci.* **2016**, *482*, 27−38.
(13) Nypelö, T. E.; Carrillo, C. A.; Rojas, O. J. Lignin supracolloids synthesized from (W/O) microemulsions: use in the interfacial stabilization of Pickering systems and organic carriers for silver metal. *Soft Matter* **2015**, *11*, 2046−2054.
(14) Ogunkoya, D.; Li, S.; Rojas, O. J.; Fang, T. Performance, combustion, and emissions in a diesel engine operated with fuel-in-water emulsions based on lignin. *Appl. Energy* **2015**, *154*, 851−861.
(15) Tzoumaki, M. V.; Moschakis, T.; Kiosseoglou, V.; Biliaderis, C. G. Oil-in-water emulsions stabilized by chitin nanocrystal particles. *Food Hydrocolloids* **2011**, *25*, 1521−1529.
(16) Wang, X.-Y.; Heuzey, M.-C. Chitosan-based conventional and Pickering emulsions with long-term stability. *Langmuir* **2016**, *32*, 929−936.
(17) Haaj, S. B.; Thielemans, W.; Magnin, A.; Boufi, S. Starch nanocrystal stabilized pickering emulsion polymerization for nanocomposites with improved performance. *ACS Appl. Mater. Interfaces* **2014**, *6*, 8263−8273.
(18) Kedzior, S. A.; Marway, H. S.; Cranston, E. D. Tailoring Cellulose Nanocrystal and Surfactant Behavior in Miniemulsion Polymerization. *Macromolecules* **2017**, *50*, 2645−2655.
(19) Hu, Z.; Marway, H. S.; Kasem, H.; Pelton, R.; Cranston, E. D. Dried and Redispersible Cellulose Nanocrystal Pickering Emulsions. *ACS Macro Lett.* **2016**, *5*, 185−189.
(20) Peddireddy, K. R.; Nicolai, T.; Benyahia, L.; Capron, I. Stabilization of Water-in-Water Emulsions by Nanorods. *ACS Macro Lett.* **2016**, *5*, 283−286.
(21) Zoppe, J. O.; Venditti, R. A.; Rojas, O. J. Pickering emulsions stabilized by cellulose nanocrystals grafted with thermo-responsive polymer brushes. *J. Colloid Interface Sci.* **2012**, *369*, 202−209.
(22) Kalashnikova, I.; Bizot, H.; Cathala, B.; Capron, I. New Pickering emulsions stabilized by bacterial cellulose nanocrystals. *Langmuir* **2011**, *27*, 7471−7479.
(23) Cherhal, F.; Cousin, F.; Capron, I. Structural description of the interface of Pickering emulsions stabilized by cellulose nanocrystals. *Biomacromolecules* **2016**, *17*, 496−502.
(24) Grishkewich, N.; Mohammed, N.; Tang, J.; Tam, K. C. Recent advances in the application of cellulose nanocrystals. *Curr. Opin. Colloid Interface Sci.* **2017**, *29*, 32−45.
(25) Carrillo, C. A.; Nypelö, T. E.; Rojas, O. J. Cellulose nanofibrils for one-step stabilization of multiple emulsions (W/O/W) based on soybean oil. *J. Colloid Interface Sci.* **2015**, *445*, 166−173.
(26) Nikfarjam, N.; Qazvini, N. T.; Deng, Y. Surfactant free Pickering emulsion polymerization of styrene in w/o/w system using cellulose nanofibrils. *Eur. Polym. J.* **2015**, *64*, 179−188.
(27) Carrillo, C. A.; Nypelö, T.; Rojas, O. J. Double emulsions for the compatibilization of hydrophilic nanocellulose with non-polar polymers and validation in the synthesis of composite fibers. *Soft Matter* **2016**, *12*, 2721−2728.
(28) Capron, I.; Rojas, O. J.; Bordes, R. Behavior of nanocelluloses at interfaces. *Curr. Opin. Colloid Interface Sci.* **2017**, *29*, 83−95.
(29) Tardy, B. L.; Yokota, S.; Ago, M.; Xiang, W.; Kondo, T.; Bordes, R.; Rojas, O. J. Nanocellulose-Surfactant Interactions. *Curr. Opin. Colloid Interface Sci.* **2017**, *29*, 57−67.
(30) Xu, X.; Wang, H.; Jiang, L.; Wang, X.; Payne, S. A.; Zhu, J.; Li, R. Comparison between cellulose nanocrystal and cellulose nanofibril reinforced poly (ethylene oxide) nanofibers and their novel shish-kebab-like crystalline structures. *Macromolecules* **2014**, *47*, 3409−3416.
(31) Habibi, Y.; Lucia, L. A.; Rojas, O. J. Cellulose nanocrystals: chemistry, self-assembly, and applications. *Chem. Rev.* **2010**, *110*, 3479−3500.
(32) Gordeyeva, K. S.; Fall, A. B.; Hall, S.; Wicklein, B.; Bergström, L. Stabilizing nanocellulose-nonionic surfactant composite foams by delayed Ca-induced gelation. *J. Colloid Interface Sci.* **2016**, *472*, 44−51.
(33) Xhanari, K.; Syverud, K.; Chinga-Carrasco, G.; Paso, K.; Stenius, P. Structure of nanofibrillated cellulose layers at the o/w interface. *J. Colloid Interface Sci.* **2011**, *356*, 58−62.
(34) Quennouz, N.; Hashmi, S. M.; Choi, H. S.; Kim, J. W.; Osuji, C. O. Rheology of cellulose nanofibrils in the presence of surfactants. *Soft Matter* **2016**, *12*, 157−164.
(35) Binks, B. P.; Murakami, R. Phase inversion of particle-stabilized materials from foams to dry water. *Nat. Mater.* **2006**, *5*, 865−869.
(36) Manova, A.; Viktorova, J.; Köhler, J.; Theiler, S.; Keul, H.; Piryazev, A. A.; Ivanov, D. A.; Tsarkova, L.; Möller, M. Multilamellar Thermoresponsive Emulsions Stabilized with Biocompatible Semicrystalline Block Copolymers. *ACS Macro Lett.* **2016**, *5*, 163−167.
(37) Klaus, A.; Tiddy, G. J.; Solans, C.; Harrar, A.; Touraud, D.; Kunz, W. Effect of salts on the phase behavior and the stability of nano-emulsions with rapeseed oil and an extended surfactant. *Langmuir* **2012**, *28*, 8318−8328.
(38) Peng, B.; Han, X.; Liu, H.; Berry, R. C.; Tam, K. C. Interactions between surfactants and polymer-grafted nanocrystalline cellulose. *Colloids Surf., A* **2013**, *421*, 142−149.
(39) Kumar, A.; Li, S.; Cheng, C.-M.; Lee, D. Recent Developments in Phase Inversion Emulsification. *Ind. Eng. Chem. Res.* **2015**, *54*, 8375−8396.
(40) Herzig, E.; White, K.; Schofield, A.; Poon, W.; Clegg, P. Bicontinuous emulsions stabilized solely by colloidal particles. *Nat. Mater.* **2007**, *6*, 966−971.
(41) Kose, R.; Kasai, W.; Kondo, T. Switching surface properties of substrates by coating with a cellulose nanofiber having a high adsorbability. *Sen'i Gakkaishi* **2011**, *67*, 163−167.
(42) Tsuboi, K.; Yokota, S.; Kondo, T. Difference between bamboo- and wood-derived cellulose nanofibers prepared by the aqueous counter collision method. *Nord. Pulp Pap. Res. J.* **2014**, *29*, 69−76.
(43) Kondo, T.; Kose, R.; Naito, H.; Kasai, W. Aqueous counter collision using paired water jets as a novel means of preparing bio-nanofibers. *Carbohydr. Polym.* **2014**, *112*, 284−290.
(44) Cifuentes, A.; Bernal, J. L.; Diez-Masa, J. C. Determination of critical micelle concentration values using capillary electrophoresis instrumentation. *Anal. Chem.* **1997**, *69*, 4271−4274.
(45) Williams, R.; Phillips, J.; Mysels, K. The critical micelle concentration of sodium lauryl sulphate at 25 °C. *Trans. Faraday Soc.* **1955**, *51*, 728−737.

DOI: 10.1021/acs.biomac.7b01452
Biomacromolecules 2017, 18, 4393−4404

(46) Tucker, I. M.; Petkov, J. T.; Penfold, J.; Thomas, R. K. Interaction of the Anionic Surfactant SDS with a Cellulose Thin Film and the Role of Electrolyte and Poyelectrolyte. 2 Hydrophilic Cellulose. *Langmuir* **2012**, *28*, 10223−10229.
(47) Kalashnikova, I.; Bizot, H.; Cathala, B.; Capron, I. Modulation of cellulose nanocrystals amphiphilic properties to stabilize oil/water interface. *Biomacromolecules* **2012**, *13*, 267−275.
(48) Hu, Z.; Ballinger, S.; Pelton, R.; Cranston, E. D. Surfactant-enhanced cellulose nanocrystal Pickering emulsions. *J. Colloid Interface Sci.* **2015**, *439*, 139−148.
(49) Gestranius, M.; Stenius, P.; Kontturi, E.; Sjöblom, J.; Tammelin, T. Phase behaviour and droplet size of oil-in-water Pickering emulsions stabilised with plant-derived nanocellulosic materials. *Colloids Surf., A* **2017**, *519*, 60−70.
(50) Cunha, A. G.; Mougel, J.-B.; Cathala, B.; Berglund, L. A.; Capron, I. Preparation of double Pickering emulsions stabilized by chemically tailored nanocelluloses. *Langmuir* **2014**, *30*, 9327−9335.

DOI: 10.1021/acs.biomac.7b01452
Biomacromolecules 2017, 18, 4393−4404